AUTHOR CORRECTION

Love, D. C., Kochran, J., Cathey, R. L., Shin, S.-H. and Hanover, J. A. (2003). Mitochondrial and nucleocytoplasmic targeting of O-linked GlcNAc transferase. *J. Cell Sci.* **116**, 647-654.

There were two errors in both the online and print versions of this paper. The second author J. Kochan was spelt incorrectly. In addition, a line was omitted from the acknowledgements. The correct author spelling and complete acknowledgement is shown below.

Mitochondrial and nucleocytoplasmic targeting of O-linked GlcNAc transferase

Dona C. Love[1], Jarema P. Kochan[2], R. Lamont Cathey[1,*], Sang-Hoon Shin[1] and John A. Hanover[1,‡]

[1]Laboratory of Cell Biochemistry and Biology, NIDDK, National Institutes of Health, Bethesda, MD, 20892, USA
[2]Department of Metabolic Diseases, Hoffman-La Roche Inc., 340 Kingsland Street, Nutley, NJ, 07110, USA
*Present address: Department of General Surgery, Carolinas Medical Center, Charlotte, NC 28232-2861, USA
‡Author for correspondence (e-mail: jah@helix.nih.gov)

The authors gratefully acknowledge William Prinz and Jenny Hinshaw for help and advice with mitochondrial subfractionation and electron microscopy, and the expert assistance of Charles Burghardt in the preparation of the OGT antibodies. The authors also thank William Lubas for helpful discussions and reagents.

Mitochondrial and nucleocytoplasmic targeting of O-linked GlcNAc transferase

Dona C. Love[1], Jarema Kochran[2], R. Lamont Cathey[1,*], Sang-Hoon Shin[1] and John A. Hanover[1,‡]

[1]Laboratory of Cell Biochemistry and Biology, NIDDK, National Institutes of Health, Bethesda, MD, 20892, USA
[2]Department of Metabolic Diseases, Hoffman-La Roche Inc., 340 Kingsland Street, Nutley, NJ, 07110, USA
*Present address: Department of General Surgery, Carolinas Medical Center, Charlotte, NC 28232-2861, USA
‡Author for correspondence (e-mail: jah@helix.nih.gov)

Accepted 31 October 2002
Journal of Cell Science 116, 647-654 © 2003 The Company of Biologists Ltd
doi:10.1242/jcs.00246

Summary

O-linked GlcNAc transferase (OGT) mediates a novel glycan-dependent signaling pathway, but the intracellular targeting of OGT is poorly understood. We examined the localization of OGT by immunofluorescence microscopy, subcellular fractionation and immunoblotting using highly specific affinity-purified antisera. In addition to the expected nuclear localization, we found that OGT was highly concentrated in mitochondria. Since the mitochondrial OGT (103 kDa) was smaller than OGT found in other compartments (116 kDa) we reasoned that it was one of two predicted splice variants of OGT. The N-termini of these isoforms are unique; the shorter form contains a potential mitochondrial targeting sequence. We found that when epitope-tagged, the shorter form (mOGT; 103 kDa) concentrated in HeLa cell mitochondria, whereas the longer form (ncOGT; 116 kDa) localized to the nucleus and cytoplasm. The N-terminus of mOGT was essential for proper targeting. Although mOGT appears to be an active transferase, O-linked GlcNAc-modified substrates do not accumulate in mitochondria. Using immunoelectron microscopy and mitochondrial fractionation, we found that mOGT was tightly associated with the mitochondrial inner membrane. The differential localization of mitochondrial and nucleocytoplasmic isoforms of OGT suggests that they perform unique intracellular functions.

Key words: OGT, O-GlcNAc, Glycan-dependent signaling, Mitochondria

Introduction

An increasing body of evidence suggests that the addition of O-linked GlcNAc by O-linked GlcNAc transferase (OGT) represents a signaling modification (Cole and Hart, 2001; Comer and Hart, 1999; Hanover, 2001; Roos and Hanover, 2000). This addition occurs at serine and threonine residues of cytosolic and nuclear proteins and, like phosphorylation, can change the function of such proteins as Sp1 and eNOS (Du et al., 2001; Yang et al., 2001). Other examples of substrates for the O-GlcNAcase are components of the nuclear pore complex (Nup 62, POM 121 and Nup180), transcription machinery (RNA polymerase II, SP1), transcription factors (c-myc, p53, and Rb) and structural proteins of the cytoplasm (cytokeratins, talin, and vinculin) (Hanover, 2001). Despite the vast array of proteins modified by OGT, these proteins share common characteristics: they are all part of macromolecular complexes and are phosphorylated and regulated throughout the cell cycle. Given the diverse substrates of OGT, understanding the structure and function of this enzyme is essential for understanding its regulation.

OGT is encoded by a single gene on the X chromosome (Akimoto et al., 1999; Kreppel et al., 1997; Lubas and Hanover, 2000; Lubas et al., 1997; Shafi et al., 2000). Gene knock-out experiments have shown that OGT is essential for stem cell viability (Hanover et al., 2002) and embryonic development (Shafi et al., 2000). OGT can be divided into three functional domains: an N-terminal tetratricopeptide region (TPR), a linker and a catalytic C-terminus. The reported OGT isoforms contain between 9-12 TPRs (Kreppel et al., 1997; Lubas and Hanover, 2000; Lubas et al., 1997). This conserved TPR domain is present in many proteins and is important for protein-protein interactions (Blatch and Lassle, 1999). Varying the number of TPR domains in OGT affects its substrate recognition (Lubas and Hanover, 2000). The linker region of OGT contains a nuclear localization sequence, consistent with a nuclear localization (Kreppel et al., 1997; Lubas et al., 1997). The proposed catalytic domain of OGT contains conserved amino acid domains that are present in other glycosyl transferases (Roos and Hanover, 2000; Wrabl and Grishin, 2001). Modest deletions in the C-terminus of OGT lead to dramatic reductions in enzymatic activity, supporting its role in catalysis (Lubas and Hanover, 2000).

The terminal product in the hexosamine biosynthetic pathway, UDP-GlcNAc, is utilized by OGT as a donor. A link between the hexosamine biosynthetic pathway and cellular glucose sensing by insulin has been established (Marshall et al., 1991; Traxinger and Marshall, 1991; Traxinger and Marshall, 1992). Further, overexpression of either the rate-limiting enzyme of the hexosamine biosynthetic pathway or OGT in the striated muscle and fat of transgenic mice leads to insulin resistance (Hebert et al., 1996; McClain et al., 2002; Tang et al., 2000; Veerababu et al., 2000). This insulin resistance was phenotypically similar to that observed in human type 2 diabetes. Additionally, recent studies have demonstrated a relationship between mitochondrial function, O-GlcNAc metabolism and maintenance of the diabetic state

(Du et al., 2000; Nishikawa et al., 2000). Therefore it is likely that OGT, by utilizing the terminal product of hexosamine biosynthesis, may mediate many of the effects attributed to the dysregulation of this pathway.

Here we report the existence of two OGT isoforms differing in their subcellular localization. The shorter form associates with mitochondria in both primary and immortilized cells, whereas the longer form is nucleocytoplasmic. The N-terminus of the short form contains mitochondrial targeting information and is essential for mitochondrial localization. These data are discussed in terms of the role of differential targeting of OGT to the mitochondrion and nucleus in the regulation of a hexosamine-dependent signaling pathway.

Materials and Methods

Plasmids

pmOGT-myc was created by inserting a PCR product containing a *Bam*HI site, Kozac consensus sequence and nucleotides spanning the atg start site to the *Xho*I site of *mogt* into pcDNA4/myc-His C (Invitrogen, Carlsbad, CA). pcnOGT-myc was created by digestion of pLKG1 (Kreppel et al., 1997), containing full-length rat cnOGT, with *Hin*dIII and *Xho*I. This purified fragment was inserted into pCDNA4myc His C (Invitrogen) using the same sites. Finally, pGFP-mOGT was created by digesting pLV4f (Lubas et al., 1997), encoding full-length mOGT, with *Eco*RV and *Bam*HI and inserting the purified fragment into the *Eco*ICR1 and *Bam*HI sites of pEGFP-C2 (Invitrogen).

Transfections

HeLa cells were seeded on glass coverslips in six-well plates (Corning Incorporated, Corning, NY) at 1×10^5 cells per well. Once cells were attached to the coverslips, they were transfected with indicated plasmids, using Fugene 6 (Roche, Indianapolis, IN) according to the manufacturer's instructions.

Antibodies

Mouse anti-Cytochrome clone 26E3, used at 2 μg/ml, and clone 7H8.2C12, used at 0.5 μg/ml, were obtained from Zymed Laboratories (South San Francisco, CA). Anti-myc clone 9E10 (Roche) was used at 2 μg/ml. Anti-mitochondrial heat shock protein 70, clone JG1 (Affinitiy Bioreagents, Golden, CO) was used at a dilution of 1:500. Anti-O-linked N-Acetlyglucosamine, clone RL2 (Affinity Bioreagents) was used at a dilution of 1:100, and CTD110.6 (Covance, Berkeley CA) was used at 1:1000. Rabbit polyclonal peptide antiserum was raised against residues 581-600 of mOGT. Affinity-purified antibodies to OGT were generated and purified according to published methods (Baskin et al., 1999; Osborne et al., 1995).

Immunolocalization

HeLa cells CCL2 (ATCC, Manassas, VA) were grown as described (Love et al., 1998). Human aortic endothelial cells (Cascade Biologics, Portland, OR) were grown and maintained according to the supplier's instructions. Cells were grown overnight on glass coverslips, then processed for immunolocalization. All cells were fixed with 4% formaldehyde (Ladd Research Industries, Williston, VT) in PBS (Mediatech, Herndon, VA) for 30 minutes at room temperature, washed three times in PBS, then permeabilized with 0.1% tritonX-100 (Calbiochem-Novabiochem Corporation, La Jolla, CA) for 3 minutes. After permeabilization, cells were washed three times in PBS and incubated with the primary antibodies for 1 hour at room temperature with gentle shaking. Primary antibodies were diluted in 5% goat serum, 2% BSA, in PBS. Following primary antibody incubation, cells were washed once for 15 minutes, then twice for 5 minutes before addition of appropriate, fluorescently conjugated, secondary antibodies (JacksonImmuno Research, West Grove, PA) for 1 hour at room temperature. Where indicated, MitoTracker® Red CM-H_2Xros (Molecular Probes, Eugene, OR) was used to label respiring mitochondria according to manufacturer's instructions. Cells were then washed three times in PBS and mounted on glass coverslips using Vectashield antifade mounting medium (Vector Laboratories, Inc., Burlingame, CA). All images were obtained using an Axiovert 200M (Carl Zeiss Inc., Thornwood, NY) with an UltraView (Perkin Elmer, Wellesley, MA) spinning disk confocal scan head. Images were captured with a Quantix back-thinned EE57 CCD camera (Roper Scientific, Trenton, NJ) with binning set at two. All images were processed using OpenLab software (Improvision, Lexington, MA).

Electron microscopy

Purified mitochondria (4C Biotech, Seneffe, Belgium) were prepared and imaged by Paragon Biotech, Inc. (Baltimore, MD). Briefly, mitochondrial pellets were fixed with either 4% paraformaldehyde or 4% paraformaldehyde with 1% glutaraldehyde in 0.1 M phosphate buffer and processed for routine TEM embedding and sectioning and mounted onto nickel grids. The grids were incubated in 3% H_2O_2 in 0.1M PB for 5-15 minutes. After several rinses in PBS, grids were blocked with 0.5% BSA, 2% normal goat serum in PBS for 30 minutes. Sections were incubated with rabbit polyclonal OGT antiserum diluted 1:50 in PBS for 1 hour. Sections were then incubated with biotinylated, goat anti-rabbit secondary antibody at 1:400 (Vector) in PBS for 30 minutes at room temperature, followed by incubation with strepavidin gold conjugate (1:20, 10 nm gold particles) for 1 hour and rinsed in distilled water. The grids were double stained with uranyl acetate and lead citrate and observed and photographed using a Zeiss electron microscope.

Biochemical isolation and separation of HeLa cells

HeLa cell subcelluar fractions were obtained from 4C Biotech. Mitochondria were separated into soluble proteins and membrane-associated proteins. Peripheral proteins were removed by incubating mitochondria in 1 M KCl for 30 minutes on ice, followed by centrifugation at 18,000 ***g*** for 30 minutes at 4°C. The mitochondrial pellet was resuspended at 30 mg/ml in 0.6 M sorbitol, 20 mM HEPES, pH 7.4, 2 mM $MgCl_2$ supplemented with Complete Mini EDTA-free protease inhibitor cocktail tablets (Roche). The mitochondrial suspension was sonicated for three 10 second pulses using an Ultrasonic Processor XL (Misonix, Inc., Farmingdale, NY). Broken mitochondria were then centrifuged for 30 minutes at 100,000 ***g*** at 4°C to separate membrane-associated and soluble proteins. The membrane-associated proteins were then solubilized in 0.2% Triton X-100. The soluble proteins contained within the supernatent were precipitated by adding 0.0125% (w/v) sodium deoxycholate, then one fifth of the volume of 72% TCA for 30 minutes and centrifuged for 30 minutes at 18,000 ***g***. Pellets were washed with ice cold acetone and recentrifuged. All pellets were resuspended in NuPAGE LDS sample buffer (Invitrogen). Mitoplasts were generated as described (Noma et al., 2001). Briefly, mitochondria were suspended in 20 mM HEPES-KOH, pH 7.4, and then placed in a test tube on ice for 30 minutes. The mitoplasts were recovered by centrifugation at 4000 ***g*** and then resuspended in 10 mM HEPES-KOH, pH 7.4, containing 220 mM mannnitol and 70 mM sucrose. Alkaline extraction with carbonate buffer was performed as described previously (Lynn et al., 2001). Briefly, mitochondria and mitoplasts were resuspended in 100 mM sodium carbonate pH 11 for 30 minutes at 4°C, then centrifuged at 100,000

g for 30 minutes. All protein determinations were performed by the BCA assay (Pierce Biotechnology, Rockford, IL).

Western blot analysis

Protein samples were separated using NuPage® Bis-Tris gels (Invitrogen) and transferred to a nitrocellulose membrane for immunoblot analysis. Briefly, nitrocellulose membranes were blocked for 1 hour at room temperature with 5% nonfat dry milk with 0.1% Tween-20 (Sigma Chemical Corporation, St. Louis, MO), in Tris-buffered saline (Quality Biological, Incorporated, Gaithersburg, MD) (TBS-T). Primary antibodies were diluted in TBS-T containing 2% nonfat dry milk and incubated with the membrane. The horseradish-peroxidase-conjugated secondary antibodies (Jackson Immuno Research) were diluted in 2% BSA, 0.1% Tween 20, PBS. All antibody incubations were conducted for 1 hour at room temperature. Washes were conducted to remove the unbound primary and secondary antibodies and consisted of two quick washes in TBS-T or PBS-T, then one 15 minute and two 5 minute washes. Membranes were visualized using the Renaissance Chemiluminescence Reagent Plus Western Blot kit (NEN™ Life Science Products, Inc., Boston, MA) according to the manufacturer's instructions.

Proteomics tools

The mitochondrial targeting sequence was predicted using iPSORT (http://www.hypothesiscreator.net/iPSORT/). The membrane-spanning region was predicted using TopPred 2 (http://bioweb.pasteur.fr/seqanal/interfaces/toppred.html).

Results

Intracellular localization of OGT isoforms

To better understand the function and regulation of OGT we examined the intracellular localization of the enzyme. We raised two highly specific rabbit polyclonal antisera and affinity purified them using recombinant human OGT. These antibodies recognize only known isoforms of OGT (see Fig. 1B, Fig. 4B,C). We then used these affinity-purified anti-OGT antibodies to detect OGT by immunofluorescence microscopy. OGT was localized to the nucleus as has been reported previously (Akimoto et al., 1999; Akimoto et al., 2000; Lubas et al., 1997) and also along cytoplasmic tubular structures suggestive of mitochondria. Dual staining of HeLa cells for OGT and for an abundant mitochondrial marker, cytochrome C oxidase, confirmed the mitochondrial localization of OGT (Fig. 1A). The merged image of OGT (green) and cytochrome C (red) revealed nearly perfect colocalization along mitochondria. In some areas, the OGT appears more punctate than did the cytochrome C (Fig. 1A). Colocalization of OGT in mitochondria was also demonstrated using mitochondrially targeted red fluorescent protein (data not shown). The mitochondrial localization of OGT was not cell type specific; a similar pattern was also detected in human aortic endothelial cells (HAEC), a primary cell line (Fig. 1A, bottom row) and in INS-1 cells (data not shown). Further verification of the mitochondrial localization of OGT was obtained using peptide antisera directed against amino acids 581-600 of OGT (data not shown). The immunofluorescent results were also verified by subcellular fractionation and immunoblotting. HeLa cells were fractionated by differential centrifugation and the subcellular fractions were examined by immunoblotting with anti-OGT. As shown in Fig. 1B, two species of OGT were detected by the antisera in total HeLa extracts. The relative levels of these two species (116 and 103 kDa) in the extract were somewhat variable and ranged from 5:1 to 1:1. When we examined the subcellular fractions, we found that the 103 kDa species was enriched in the mitochondrial fraction (mito) whereas the 116 kDa species was preferentially found in the nuclear fraction (nuclear). Densitometry of the bands in each of the fractions demonstrated that the ratio of 103 kDa to 116 kDa species was ~10-fold higher in the mitochondrial fraction, indicating significant enrichment of the 103 kDa species in the mitochondria. A similar enrichment of the mitochondrial marker, cytochrome c, was observed in this fraction (~12 fold; data not shown). Therefore, both our immunofluorescence and immunoblotting results suggested that

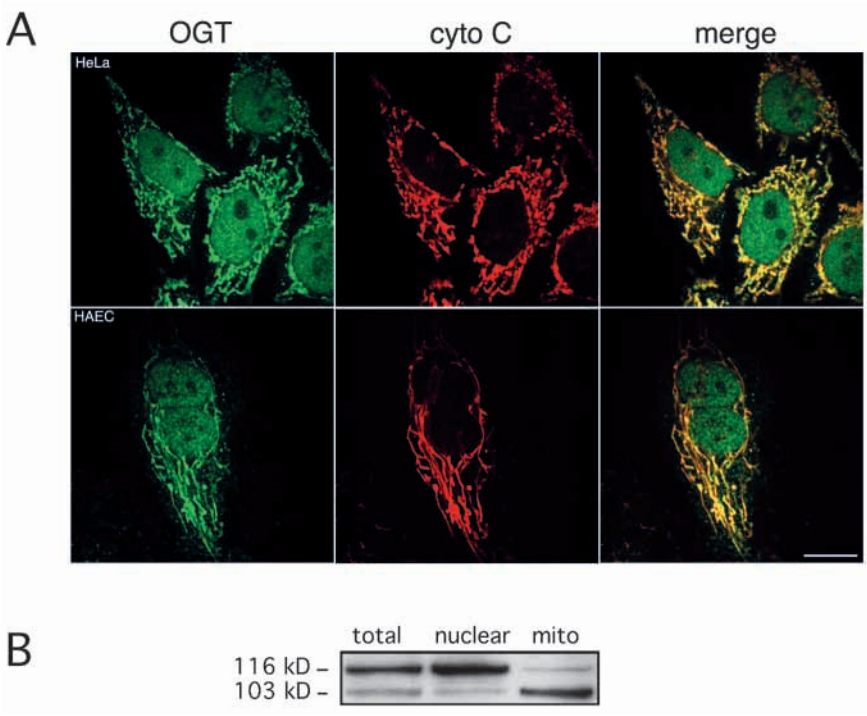

Fig. 1. Nucleocytoplasmic and mitochondrial localization of OGT. (A) HeLa cells (top row) and HAEC (bottom row) were grown on glass coverslips, fixed and processed for indirect immunofluorescence using affinity-purified anti-OGT antibodies and a mouse monoclonal antibody raised against cytochrome C. The confocal images representing OGT (green) and cytochrome C (red) were overlayed (merge) to reveal colocalization. Bar, 10 µM. (B) Total cellular lysate (total), nuclear and mitochondrial (mito) fractions from HeLa cells were separated using a 10% PAGE-gel, transferred to nitrocellulose and probed with OGT-specific, affinity-purified antibodies as described in Materials and Methods. Equal amounts of protein were loaded in each lane. Note the enrichment (~10-fold) of the 103 kDa species in mitochondria.

distinct forms of OGT reside in the nucleus and mitochondria; little OGT was found free in the cytoplasm.

Targeting information in OGT isoforms

In contrast to the expected nuclear localization of OGT, the striking mitochondrial localization we observed was surprising. The findings further suggested that the 103 kDa mitochondrial form of the enzyme might represent a distinct biochemical species (Fig. 1B). Several isoforms of OGT have been described which seem to arise by alternative splicing of the mammalian *ogt* gene (Kreppel et al., 1997; Lubas et al., 1997; Nolte and Muller, 2002; Hanover et al., 2002). These known isoforms include species with predicted molecular weights of 116 (Kreppel et al., 1997) and 103 kDa (Lubas et al., 1997). We utilized several web-based search tools to identify regions of OGT that might target either of these isoforms to mitochondria. iPSORT identified a 20 amino-acid stretch at the unique N-terminal end of the 103 kDa isoform, which we designate mOGT (mitochondrial OGT) (Lubas et al., 1997), as the mitochondrial targeting sequence (Fig. 2A, bottom row). Interestingly, this mitochondrial targeting sequence was detected only when mOGT was designated as a plant protein, suggesting that this mitochondrial targeting sequence is somewhat unusual. The longer isoform of OGT, which we designate ncOGT (nucleocytoplasmic OGT) (Kreppel et al., 1997), did not contain a mitochondrial targeting sequence; instead, ncOGT contains a unique N-terminus and three additional TPRs when compared to mOGT (Fig. 2A, top row). Efforts to produce antipeptide antisera to distinguish between the two isoforms proved difficult. Therefore, to examine the targeting of these two OGT isoforms we expressed myc-tagged versions of m OGT and ncOGT (Fig. 2B). As we had previously documented that expressing the full-length, catalytically active mOGT was quite toxic (Lubas et al., 1997), we replaced the last 93 amino acids of the catalytic domains of ncOGT and mOGT with myc tags. We have previously shown that this deletion inactivates the catalytic activity of OGT (Lubas and Hanover, 2000). Immunolocalization of myc-tagged ncOGT indicated a somewhat diffuse pattern distributed throughout the nucleus and cytoplasm with no enrichment in mitochondria (Fig. 2Ba). By contrast, mOGT was associated with cytoplasmic structures highly suggestive of mitochondria (Fig. 2Bb). This localization was not eptitope-tag-specific; the same localization pattern was observed when GFP was used instead of the myc epitope (data not shown). The importance of the N-terminus of mOGT for this unique targeting was demonstrated by deletional analysis. Removal of the first

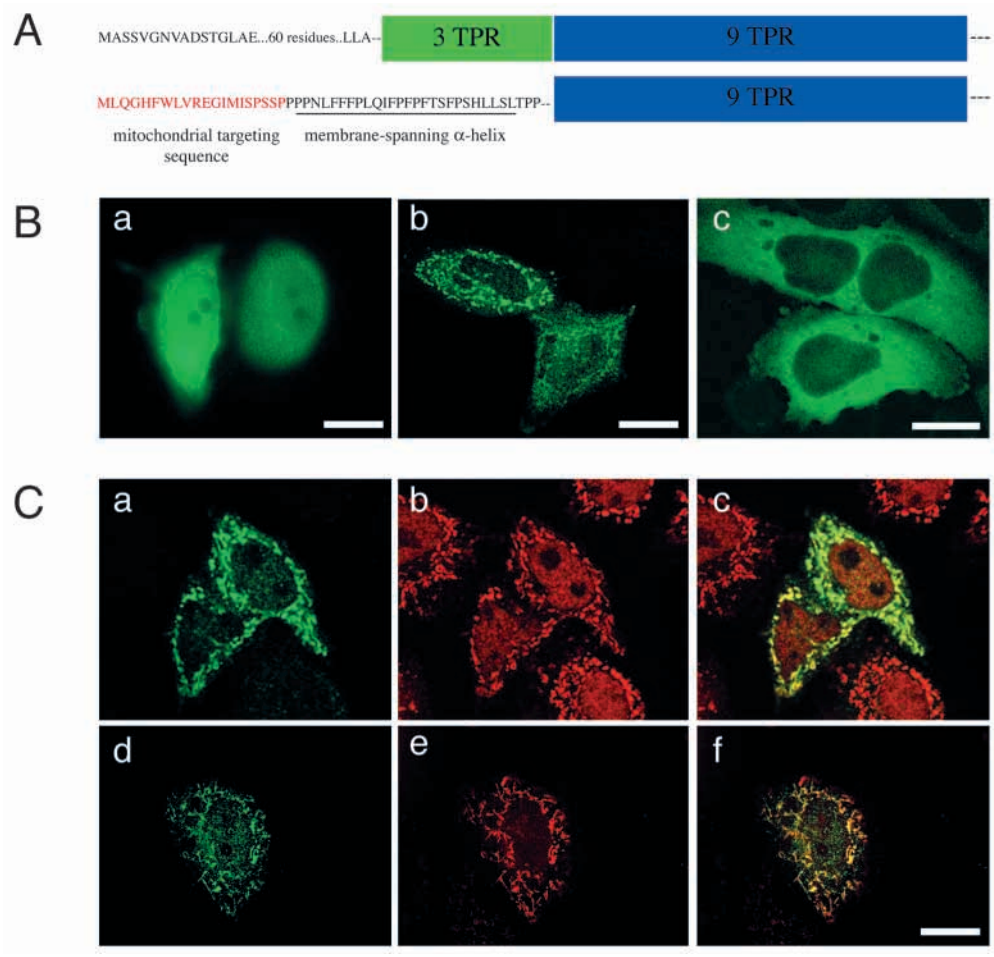

Fig. 2. Identification of nucleocytoplasmic and mitochondrial isoforms of OGT. (A) A schematic of known OGT isoforms is shown to illustrate the unique N-termini. ncOGT (top row) contains 89 amino acids and an additional three TPRs, compared to mOGT (bottom row). mOGT contains a putative mitochondrial targeting sequence at its N-terminus (shown in red) and a predicted membrane-spanning helix (underlined). Both OGT isoforms are identical from the nine TPR region to their C-termini. (B) The 116 kDa (ncOGT) and 103 kDa (mOGT) isoforms of OGT were expressed in HeLa cells as a C-terminus myc-fusion. 24 hours following transfection cells were fixed and processed for indirect immunofluorescence using an anti-myc monoclonal antibody (a and b). ncOGT was distributed between the nucleus and cytoplasm and did not accumulate in mitochondria (Ba). By contrast, mOGT concentrated in cytoplasmic structures highly reminiscent of mitochondria (Bb; see below). The third panel (Bc) shows the cytoplasmic localization of GFP-ΔmOGT, which lacks the mitochondrial targeting region of mOGT. (C) The myc-tagged mOGT (Ca) colocalized with anti-OGT antibodies (Cb), which recognize both OGT isoforms. Colocalization was apparent only in the mitochondria; the tagged mOGT did not significantly colocalize with the endogenous nuclear OGT (Cc). The lower panels (Cd-f) show colocalization of mOGT (Cd) with MitoTracker® Red CM-H_2XRos (Ce), a mitochondrial marker. The merged image shows colocalization in mitochondria (Cf). Bars, 10 μM.

15 amino acids of mOGT (GFP-ΔmOGT) prevented concentration in mitochondria and resulted in a primarily cytoplasmic localization, with a small amount found in the nucleus (Fig. 2Bc).

The N-terminus of mOGT is important for mitochondrial targeting

To confirm that the mOGT isoform is uniquely targeted to mitochondria, we colocalized myc-tagged mOGT with both endogenous OGT and with a mitochondrion-selective probe (Fig. 2C). As shown in the top panels, the myc-tagged mOGT colocalizes with the endogenous mitochondrial OGT, while showing little if any colocalization with the endogenous, nuclear OGT (Fig. 2Ca-c). The myc-tagged mOGT also colocalized with MitoTracker® Red CM-H_2XRos, directly demonstrating mitochondrial targeting (Fig. 2Cd-f). Taken together, these data suggest that the unique N-terminus of mOGT contains targeting information essential for mitochondrial localization of mOGT.

O-GlcNAc-modified substrates do not accumulate in mitochondria

Although mOGT clearly localizes to mitochondria, biochemical and morphological findings suggest that only low levels of O-GlcNAc-modified substrates reside in mitochondria. As shown in Fig. 3A, when endogenous mitochondrial OGT (green) was colocalized with intracellular O-GlcNAc-modified proteins (red), no colocalization (yellow) was observed in the mitochondria. By contrast, nuclear OGT (Fig. 3A, green) and nuclear O-GlcNAc-modified proteins (Fig. 3A, red) show many areas of punctate localization. Another approach to visualizing the O-GlcNAc-modified proteins was taken by probing HeLa subcellular fractions with a monoclonal antibody (RL2) specific for O-GlcNAc-modified proteins (Fig. 3B). Multiple proteins ranging from 60 kDa to approximately 200 kDa were detected by RL2 and another monoclonal antibody CTD 110.6 (data not shown). These proteins were differentially enriched in the cytoplasm and nuclear fractions (Fig. 3B, cyto, nuc). The mitochondrial fraction, in comparison, was blank (Fig. 3B, mito). Only extreme overexposure of the western blot revealed very faint bands in the mitochondrial fraction (data not shown). Previous reports have shown that mitochondria contain the lowest amounts of cellular O-GlcNAc-modified proteins (Hanover et al., 1987; Holt and Hart, 1986). Taken together, these findings suggest that either mitochondrial OGT is catalytically inactive in this organelle or the substrates for OGT are very limited in mitochondria.

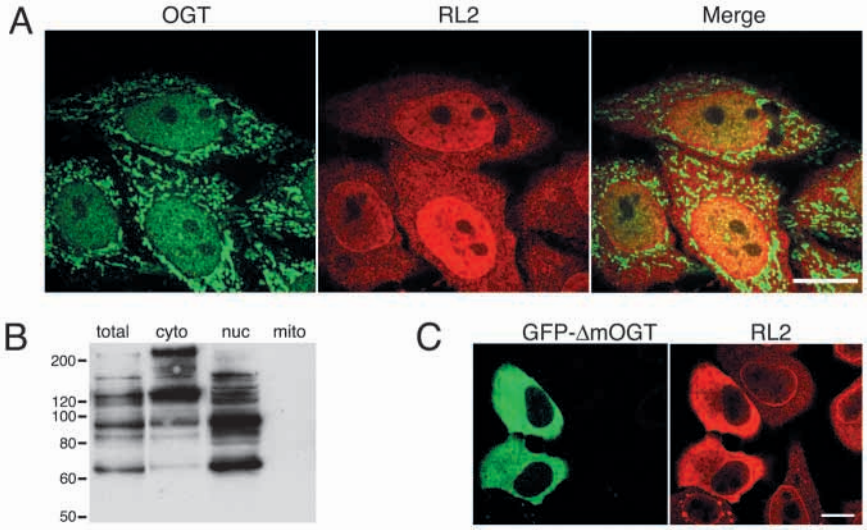

Fig. 3. O-GlcNAc-modified glycoproteins do not accumulate in mitochondria although mOGT is catalytically active. (A) Untransfected HeLa cells (upper row) were grown on glass coverslips, fixed and processed for indirect immunofluorescence to reveal endogenous OGT (OGT) and O-GlcNAc (RL2) localization. The two images were overlaid to determine colocalization (Merge). (B) HeLa subcellular fractions were probed for the O-GlcNAc-modified proteins. Equal amounts of total HeLa lysate (total), cytosol (cyto), nuclear (nuc) and mitochondrial proteins were separated using a 10% Bis-Tris SDS gel, transferred to nitrocellulose and probed with the RL2 monoclonal antibody. The migration of molecular weight markers (kDa) is shown on the left. (C) To demonstrate that mOGT is catalytically active when mislocalized from mitochondria to the cytoplasm, HeLa cells were transfected with GFP-ΔmOGT for 24 hours, fixed and processed to visualize GFP-ΔmOGT. Indirect immunofluorescence was used to localize O-GlcNAc (RL2). Bars, 10 μM.

mOGT and catalytic activity

To demonstrate that the mOGT is capable of catalytic activity, we performed two kinds of experiments. First, we showed that mOGT is catalytically active when expressed in *E. coli* (Lubas and Hanover, 2000). Second, we replaced the mitochondrial targeting sequence of mOGT with GFP (GFP-ΔmOGT, see above) and expressed the protein in HeLa cells (Fig. 3C). GFP-ΔmOGT is not targeted to mitochondria but resides mainly in the cytoplasm, with trace amounts detected in the nucleus (Fig. 3C, GFP-ΔmOGT). Staining these transfected cells with RL2 showed enhanced glycosylation in the cytoplasm of cells overexpressing GFP-ΔmOGT (Fig. 3C, RL2). Taken together, these studies argue that mitochondrial OGT, although potentially active, is sequestered from the more abundant substrates found in the nucleus and cytoplasm.

Association of mOGT with the mitochondrial membrane

To determine the mitochondrial localization of OGT at higher resolution, purified HeLa cell mitochondria were examined by indirect immunogold electron microscopy using affinity-purified anti-OGT (Fig. 4A). We determined that approximately 75% of the total gold particles were associated with the mitochondrial membrane. Upon examining a large number of labeled mitochondria, the majority of the gold label was associated with the mitochondrial inner membrane (Fig. 4A). By contrast, when a control incubation was performed (Fig. 4A,

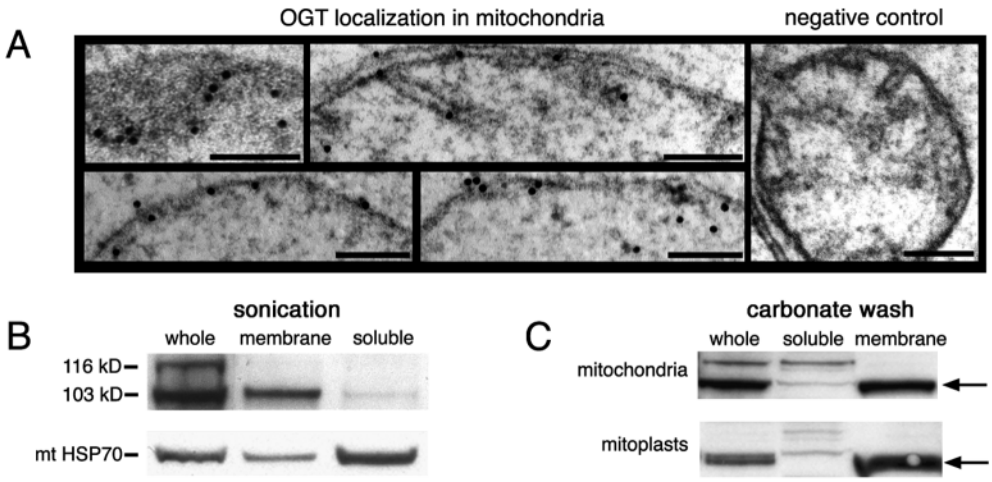

Fig. 4. OGT is associated with the mitochondrial inner membrane. (A) Immunogold staining of purified mitochondria demonstrates an inner membrane localization for OGT; no specific label was detected when the gold-labeled secondary antibody was used alone (negative control). Bars, 0.1 μM. (B) Purified HeLa mitochondria (whole) were fractionated by sonication and high-speed centrifugation into membrane and soluble protein fractions, separated on a 4-20% PAGE-gel, transferred to nitrocellulose and probed with OGT-specific, affinity-purified antibodies. Equal amounts of protein were loaded in each lane. The majority of mOGT was found associated with the membrane fraction after salt washing (see Materials and Methods). Fractionation of mitochondria was monitored by mtHSP 70 content. The bulk of this matrix marker appeared in the soluble fraction under conditions where mOGT remained membrane associated. (C) Localization of mOGT was compared in mitochondria and mitoplasts subjected to alkaline extraction with carbonate buffer. The outer membrane of mitochondria was removed by hypotonic lysis to produce the mitoplasts. Both mitochondria and the mitoplasts were washed with 100 mM sodium carbonate pH 11 to remove peripherally associated proteins. The soluble and membrane fractions were separated and probed for OGT. The arrows indicate that the mOGT is greatly enriched in the membrane fractions of both mitochondria and mitoplasts.

negative control) very little mitochondrial label was detected. Our morphometric analysis suggested that, on average, 13.4 gold particles were associated with each mitochondrion versus 0.64 gold particles per mitochondrion in the negative control. These data suggest that OGT preferentially associates with the mitochondrial inner membrane.

We used biochemical fractionation of isolated HeLa cell mitochondria and western blot analysis to corroborate the electron microscopy findings. HeLa mitochondria were fractionated into membrane-associated and soluble proteins by sonication and high-speed centrifugation (Fig. 4B). As we demonstrated in Fig. 1B, the 103 kDa mOGT species was enriched more than 10-fold in the mitochondria relative to the 116 kDa form (Fig. 4B, whole). Upon further fractionation of the mitochondria, mOGT was enriched in the salt-resistant membrane fraction (Fig. 4B, membrane). Little mOGT was present in the salt-extractable soluble fraction (Fig. 4B, soluble). The bottom row demonstrates that mitochondrial hsp70 (a matrix marker) is largely removed from the membrane fraction. To confirm the inner membrane localization, mitoplasts were made by hypotonic lysis of mitochondria. The localization of OGT was then compared in whole mitochondria and mitoplasts following a carbonate wash to remove proteins peripherally associated with the membrane (Fig. 4C). mOGT was found almost exclusively in the membrane fraction of both mitochondria and mitoplasts (Fig. 4C, arrows). Taken together, these data are consistent with the immunogold microscopic evidence, suggesting that mOGT is tightly associated with the mitochondrial inner membrane.

The sequence adjacent to the presumptive mitochondrial targeting of mOGT is quite hydrophobic and is predicted to be a membrane-spanning region using a number of algorithms (Fig. 2A, underlined). The data presented here are consistent with a tight association of the mOGT isoform to the mitochondrial inner membrane. Although the algorithms used predict that mOGT is mainly oriented toward the intermembrane space, further in vitro studies are required to confirm this localization. These findings are intriguing in light of early reports from our laboratory (Lubas et al., 1995; Lubas et al., 1997; Starr and Hanover, 1990) and the Hart laboratory (Haltiwanger et al., 1992) suggesting that both soluble and membrane-bound OGT activities were detected. This mitochondrially sequestered form of OGT (mOGT) is likely to represent the membrane-bound form of OGT reported earlier.

Discussion

We demonstrate the differential localization of two OGT isoforms, ncOGT and mOGT. The longer 116 kDa isoform (ncOGT) resides mainly in the nucleus, whereas the shorter 110 kDa (mOGT) isoform targets to mitochondria. The divergent N-terminus of mOGT contains mitochondrial targeting information that is essential for appropriate localization of mOGT. Immunolocalization and biochemical evidence suggests that mOGT associates with the mitochondrial inner membrane. The subcellular targeting of OGT implies that these isoforms perform different functions and allows for the integration of glucose sensing into different cellular pathways.

The regulation of the differing OGT isoforms

Our recent analysis of the mouse, rat (Hanover et al., 2002) and the human (Nolte and Muller, 2002) *ogt* gene suggests that the isoforms we have designated mOGT and ncOGT arise by alternative splicing from a single gene on the X-chromosome. The mOGT form utilizes intron 4 of ncOGT as an exon to generate its unique 5′ N-terminus. Interestingly, this intronic region of the *ogt* gene may also serve as an internal promoter driving the expression of only the mOGT isoform. Thus, the current evidence suggests that the two isoforms of OGT may be independently regulated. The mOGT and ncOGT isoforms

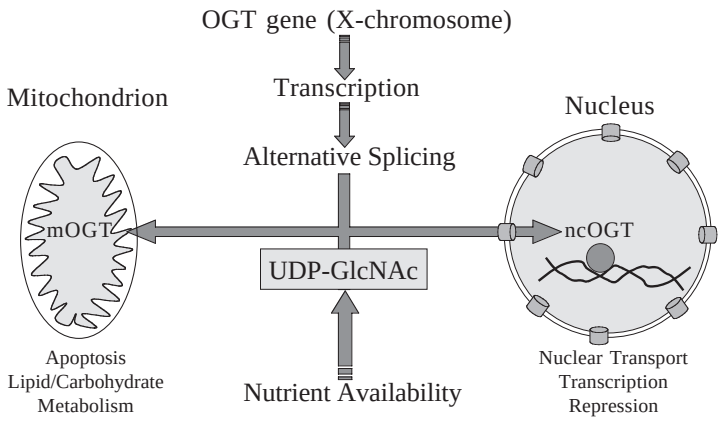

Fig. 5. A model depicting the role of differentially targeted OGT isoforms in glycan-dependent signaling. The studies described here suggest that transcription from the OGT gene and subsequent alternative splicing produces a number of isoforms including mOGT and ncOGT. The unique N-termini of these isoforms lead to segregation of mOGT into the mitochondrial membrane and targeting of ncOGT to the nucleus and cytoplasm. The hexosamine-signaling pathway is known to modulate the levels of UDP-GlcNAc in response to nutrients (glucose, glutamine, free fatty acids). The UDP-GlcNAc would then be used by each of the uniquely targeted OGT isoforms to modify different intracellular substrates. In the mitochondrion, mOGT may play a role in apoptosis and lipid and carbohydrate metabolism (see text). In the nucleus and cytosol, ncOGT is envisioned to mediate effects on translation, nuclear transport and transcriptional repression.

differ in a number of key respects. First, they differ in localization as we have demonstrated in this study. Second, they differ in the number of TPR motifs present; mOGT has nine repeats whereas the ncOGT has 12. Third, the unique N-termini of the two proteins may contain additional regulatory information unrelated to targeting. Given these differences, it is likely that the two OGT isoforms have very different substrates and intracellular functions.

Functional significance of OGT isoforms

O-GlcNAc addition and removal is dynamic and exhibits a complex interrelationship with protein phosphorylation. The O-GlcNAc modification has been implicated in a large number of diverse intracellular processes ranging from translational control, transcription, transcriptional repression, insulin resistance and regulation of the cell cycle (Hanover, 2001; Wells et al., 2001). These functions may have as a common theme the requirement for nutrient sensing and signaling through the hexosamine biosynthetic pathway (the hexosamine signaling pathway) (Hanover, 2001; Wells et al., 2001). Although the TPR domain of OGT is capable of interacting with many proteins, it is difficult to understand how one enzyme derived from a single gene could mediate such diverse intracellular functions. The model shown in Fig. 5 summarizes how the differentially targeted isoforms may contribute to hexosamine-dependent intracellular signaling. Transcripts derived from a single mammalian OGT gene on chromosome X are alternatively spliced to produce mOGT and ncOGT. The mOGT and ncOGT isoforms are likely to perform unique functions in the mitochondrion and nucleus in response to changing levels of a common precursor: UDP-GlcNAc. The mitochondrial mOGT may participate in such functions as apoptosis and the regulation of precursor transport and carbohydrate metabolism. The hexosamine pathway has been previously implicated in the regulation of apoptosis (Boehmelt et al., 2000; Hanover et al., 1999; Liu et al., 2000). In addition, we have shown that when overexpressed, the mOGT is highly toxic to cells (Lubas et al., 1997). By contrast, overexpression of ncOGT is not overtly cytotoxic (Kreppel et al., 1997) (J.A.H., unpublished). A clear relationship also exists between mitochondrial superoxide overproduction and O-GlcNAc metabolism (Du et al., 2000; Du et al., 2001; Nishikawa et al., 2000). The mOGT isoform is, therefore, likely to participate in the hexosamine-dependent changes in mitochondrial function in response to lipid and carbohydrate metabolism or proapoptotic signals.

The unique N-terminus, additional TPRs and nucleocytoplasmic localization of ncOGT suggests that this isoform participates in the cytoplasmic and nuclear events attributed to O-GlcNAc such as translation, nuclear transport, transcriptional repression and chromatin remodeling (Datta et al., 1989; Hanover, 2001; Kelly and Hart, 1989; Wells et al., 2001). Most recently, ncOGT was shown to interact with the histone deacetylation complex by binding to the corepressor mSin3a (Yang et al., 2002). By appropriate targeting of ncOGT by mSin3a, transcription can be negatively regulated through glycosylation and deacetylation. Therefore, the identification and characterization of the differentially targeted isoforms of OGT presented here should facilitate further dissection of the regulation of their unique intracellular functions.

The authors gratefully acknowledge William Prinz and Jenny Hinshaw for help and advice with mitochondrial subfractionation and electron microscopy. The authors also thank William Lubas for helpful discussions and reagents.

References

Akimoto, Y., Kreppel, L. K., Hirano, H. and Hart, G. W. (1999). Localization of the O-linked N-acetylglucosamine transferase in rat pancreas. *Diabetes* **48**, 2407-2413.

Akimoto, Y., Kreppel, L. K., Hirano, H. and Hart, G. W. (2000). Increased O-GlcNAc transferase in pancreas of rats with streptozotocin-induced diabetes. *Diabetologia* **43**, 1239-1247.

Baskin, D. G., Schwartz, M. W., Seeley, R. J., Woods, S. C., Porte, D. J., Breininger, J. F., Jonak, Z., Schaefer, J., Krouse, M., Burghardt, C. et al. (1999). Leptin receptor long-form splice-variant protein expression in neuron cell bodies of the brain and co-localization with neuropeptide Y mRNA in the arcuate nucleus. *J. Histochem. Cytochem.* **47**, 353-362.

Blatch, G. L. and Lassle, M. (1999). The tetratricopeptide repeat: a structural motif mediating protein-protein interactions. *Bioessays* **21**, 932-939.

Boehmelt, G., Wakeham, A., Elia, A., Sasaki, T., Plyte, S., Potter, J., Yang, Y., Tsang, E., Ruland, J., Iscove, N. N. et al. (2000). Decreased UDP-GlcNAc levels abrogate proliferation control in EMeg32-deficient cells. *EMBO J.* **19**, 5092-5104.

Cole, R. N. and Hart, G. W. (2001). Cytosolic O-glycosylation is abundant in nerve terminals. *J. Neurochem.* **79**, 1080-1089.

Comer, F. I. and Hart, G. W. (1999). O-GlcNAc and the control of gene expression. *Biochim. Biophys. Acta.* **1473**, 161-171.

Datta, B., Ray, M. K., Chakrabarti, D., Wylie, D. E. and Gupta, N. K. (1989). Glycosylation of eukaryotic peptide chain initiation factor 2 (eIF-2)-associated 67-kDa polypeptide (p67) and its possible role in the inhibition

of eIF-2 kinase-catalyzed phosphorylation of the eIF-2 alpha-subunit. *J. Biol. Chem.* **264**, 20620-20624.

Du, X. L., Edelstein, D., Rossetti, L., Fantus, I. G., Goldberg, H., Ziyadeh, F., Wu, J. and Brownlee, M. (2000). Hyperglycemia-induced mitochondrial superoxide overproduction activates the hexosamine pathway and induces plasminogen activator inhibitor-1 expression by increasing Sp1 glycosylation. *Proc. Natl. Acad. Sci. USA* **97**, 12222-12226.

Du, X. L., Edelstein, D., Dimmeler, S., Ju, Q., Sui, C. and Brownlee, M. (2001). Hyperglycemia inhibits endothelial nitric oxide synthase activity by posttranslational modification at the Akt site. *J. Clin. Invest.* **108**, 1341-1348.

Haltiwanger, R. S., Blomberg, M. A. and Hart, G. W. (1992). Glycosylation of nuclear and cytoplasmic proteins. Purification and characterization of a uridine diphospho-N-acetylglucosamine:polypeptide beta-N-acetylglucosaminyltransferase. *J. Biol. Chem.* **267**, 9005-9013.

Hanover, J. A. (2001). Glycan-dependent signaling: O-linked N-acetylglucosamine. *FASEB J.* **15**, 1865-1876.

Hanover, J. A., Cohen, C. K., Willingham, M. C. and Park, M. K. (1987). O-linked N-acetylglucosamine is attached to proteins of the nuclear pore. Evidence for cytoplasmic and nucleoplasmic glycoproteins. *J. Biol. Chem.* **262**, 9887-9894.

Hanover, J. A., Lai, Z., Lee, G., Lubas, W. A. and Sato, S. M. (1999). Elevated O-linked N-acetylglucosamine metabolism in pancreatic beta-cells. *Arch. Biochem. Biophys.* **362**, 38-45.

Hanover, J. A., Yu, S., Lubas, W. A., Shin, S. H., Ragano-Caracciola, M., Kochran, J. and Love, D. C. (2002). Mitochondrial and nucleocytoplasmic isoforms of O-linked GlcNAc Transferase (OGT) encoded by a single mammalian gene. *Arch Biochem Biophys.* (in press).

Hebert, L. F., Daniels, M. C., Zhou, J., Crook, E. D., Turner, R. L., Simmons, S. T., Neidigh, J. L., Zhu, J. S., Baron, A. D. and McClain, D. A. (1996). Overexpression of glutamine:fructose-6-phosphate amidotransferase in transgenic mice leads to insulin resistance. *J. Clin. Invest.* **98**, 930-936.

Holt, G. D. and Hart, G. W. (1986). The subcellular distribution of terminal N-acetylglucosamine moieties. Localization of a novel protein-saccharide linkage, O-linked GlcNAc. *J. Biol. Chem.* **261**, 8049-8057.

Kelly, W. G. and Hart, G. W. (1989). Glycosylation of chromosomal proteins: localization of O-linked N-acetylglucosamine in *Drosophila* chromatin. *Cell* **57**, 243-251.

Kreppel, L. K., Blomberg, M. A. and Hart, G. W. (1997). Dynamic glycosylation of nuclear and cytosolic proteins. Cloning and characterization of a unique O-GlcNAc transferase with multiple tetratricopeptide repeats. *J. Biol. Chem.* **272**, 9308-9315.

Liu, K., Paterson, A. J., Chin, E. and Kudlow, J. E. (2000). Glucose stimulates protein modification by O-linked GlcNAc in pancreatic beta cells: linkage of O-linked GlcNAc to beta cell death. *Proc. Natl. Acad. Sci. USA* **97**, 2820-2825.

Love, D. C., Sweitzer, T. D. and Hanover, J. A. (1998). Reconstitution of HIV-1 rev nuclear export: independent requirements for nuclear import and export. *Proc. Natl. Acad. Sci. USA* **95**, 10608-10613.

Lubas, W. A., Frank, D. W., Krause, M. and Hanover, J. A. (1997). O-linked GlcNAc transferase is a conserved nucleocytoplasmic protein containing tetratricopeptide repeats. *J. Biol. Chem.* **272**, 9316-9324.

Lubas, W. A. and Hanover, J. A. (2000). Functional expression of O-linked GlcNAc transferase. Domain structure and substrate specificity. *J. Biol. Chem.* **275**, 10983-10988.

Lubas, W. A., Smith, M., Starr, C. M. and Hanover, J. A. (1995). Analysis of nuclear pore protein p62 glycosylation. *Biochemistry* **34**, 1686-1694.

Lynn, B. D., Turley, E. A. and Nagy, J. I. (2001). Subcellular distribution, calmodulin interaction, and mitochondrial association of the hyaluronan-binding protein RHAMM in rat brain. *J. Neurosci. Res.* **65**, 6-16.

Marshall, S., Bacote, V. and Traxinger, R. R. (1991). Discovery of a metabolic pathway mediating glucose-induced desensitization of the glucose transport system. Role of hexosamine biosynthesis in the induction of insulin resistance. *J. Biol. Chem.* **266**, 4706-4712.

McClain, D. A., Lubas, W. A., Cooksey, R. C., Hazel, M., Parker, G. J., Love, D. C. and Hanover, J. A. (2002). Altered glycan-dependent signaling induces insulin resistance and hyperleptinemia. *Proc. Natl. Acad. Sci. USA* **99**, 10695-10699.

Nishikawa, T., Edelstein, D., Du, X. L., Yamagishi, S., Matsumura, T., Kaneda, Y., Yorek, M. A., Beebe, D., Oates, P. J., Hammes, H. P. et al. (2000). Normalizing mitochondrial superoxide production blocks three pathways of hyperglycaemic damage. *Nature* **404**, 787-790.

Nolte, D. and Muller, U. (2002). Human O-GlcNAc transferase (OGT): genomic structure, analysis of splice variants, fine mapping in Xq13.1. *Mamm. Genome* **13**, 62-64.

Noma, T., Fujisawa, K., Yamashiro, Y., Shinohara, M., Nakazawa, A., Gondo, T., Ishihara, T. and Yoshinobu, K. (2001). Structure and expression of human mitochondrial adenylate kinase targeted to the mitochondrial matrix. *Biochem. J.* **358**, 225-232.

Osborne, M. A., Dalton, S. and Kochan, J. P. (1995). The yeast tribrid system–genetic detection of trans-phosphorylated ITAM-SH2-interactions. *Biotechnology (NY)* **13**, 1474-1478.

Roos, M. D. and Hanover, J. A. (2000). Structure of O-linked GlcNAc transferase: mediator of glycan-dependent signaling. *Biochem. Biophys. Res. Commun.* **271**, 275-280.

Shafi, R., Iyer, S. P., Ellies, L. G., O'Donnell, N., Marek, K. W., Chui, D., Hart, G. W. and Marth, J. D. (2000). The O-GlcNAc transferase gene resides on the X chromosome and is essential for embryonic stem cell viability and mouse ontogeny. *Proc. Natl. Acad. Sci. USA* **97**, 5735-5739.

Starr, C. M. and Hanover, J. A. (1990). Glycosylation of nuclear pore protein p62. Reticulocyte lysate catalyzes O-linked N-acetylglucosamine addition in vitro. *J. Biol. Chem.* **265**, 6868-6873.

Tang, J., Neidigh, J. L., Cooksey, R. C. and McClain, D. A. (2000). Transgenic mice with increased hexosamine flux specifically targeted to beta-cells exhibit hyperinsulinemia and peripheral insulin resistance. *Diabetes* **49**, 1492-1499.

Traxinger, R. R. and Marshall, S. (1991). Coordinated regulation of glutamine:fructose-6-phosphate amidotransferase activity by insulin, glucose, and glutamine. Role of hexosamine biosynthesis in enzyme regulation. *J. Biol. Chem.* **266**, 10148-10154.

Traxinger, R. R. and Marshall, S. (1992). Insulin regulation of pyruvate kinase activity in isolated adipocytes. Crucial role of glucose and the hexosamine biosynthesis pathway in the expression of insulin action. *J. Biol. Chem.* **267**, 9718-9723.

Veerababu, G., Tang, J., Hoffman, R. T., Daniels, M. C., Hebert, L. F. J., Crook, E. D., Cooksey, R. C. and McClain, D. A. (2000). Overexpression of glutamine: fructose-6-phosphate amidotransferase in the liver of transgenic mice results in enhanced glycogen storage, hyperlipidemia, obesity, and impaired glucose tolerance. *Diabetes* **49**, 2070-2078.

Wells, L., Vosseller, K. and Hart, G. W. (2001). Glycosylation of nucleocytoplasmic proteins: signal transduction and O-GlcNAc. *Science* **291**, 2376-2378.

Wrabl, J. O. and Grishin, N. V. (2001). Homology between O-linked GlcNAc transferases and proteins of the glycogen phosphorylase superfamily. *J. Mol. Biol.* **314**, 365-374.

Yang, X., Zhang, F. and Kudlow, J. E. (2002). Recruitment of O-GlcNAc transferase to promoters by corepressor mSin3A: coupling protein O-GlcNAcylation to transcriptional repression. *Cell* **110**, 69-80.

Yang, X., Su, K., Roos, M. D., Chang, Q., Paterson, A. J. and Kudlow, J. E. (2001). O-linkage of N-acetylglucosamine to Sp1 activation domain inhibits its transcriptional capability. *Proc. Natl. Acad. Sci. USA* **98**, 6611-6616.